Vibrational spectroscopic study of the protic ionic liquid 1-H-3-methylimidazolium bis(trifluoromethanesulfonyl)imide

ARTICLE *in* VIBRATIONAL SPECTROSCOPY · NOVEMBER 2012

Impact Factor: 2 · DOI: 10.1016/j.vibspec.2012.08.006

4 AUTHORS, INCLUDING:

Anastasia Maria Moschovi
Institute of Chemical Reaction Engineering
9 PUBLICATIONS **84** CITATIONS
SEE PROFILE

Spyridon Ntais
University of Ottawa
35 PUBLICATIONS **229** CITATIONS
SEE PROFILE

Vassilios Dracopoulos
Foundation for Research and Technology -…
72 PUBLICATIONS **833** CITATIONS
SEE PROFILE

Vibrational Spectroscopy 63 (2012) 350–359

Contents lists available at SciVerse ScienceDirect

Vibrational Spectroscopy

journal homepage: www.elsevier.com/locate/vibspec

Vibrational spectroscopic study of the protic ionic liquid 1-H-3-methylimidazolium bis(trifluoromethanesulfonyl)imide

Anastasia Maria Moschovi[a,b], Spyridon Ntais[b,1], Vassilios Dracopoulos[b,*], Vladimiros Nikolakis[b,*,2]

[a] Department of Chemical Engineering, University of Patras, Greece
[b] Foundation for Research & Technology Hellas, Institute of Chemical Engineering Sciences, FORTH/ICEHT, Greece

ARTICLE INFO

Article history:
Received 17 April 2012
Received in revised form 7 August 2012
Accepted 8 August 2012
Available online 20 August 2012

Keywords:
Protic
Ionic liquid
Raman
FTIR
1-H-3-methyl imidazolium-bis(trifluoromethanesulfonyl)imide
Enthalpy
TFSI

ABSTRACT

The solid and liquid phase vibrational spectra (Raman and FTIR/ATR) of 1-H-3-methylimidazolium bis(trifluoromethanesulfonyl)imide (HMImTFSI) ionic liquid were recorded at temperatures up to 150 °C. The interpretation of the spectra indicates the existence of ion pairs in the liquid state in which, the anion and the cation, are bridged mainly through hydrogen bonds HBs between the nitrogen of the imidazole ring and the oxygen atoms of $TFSI^-$ anion. At room temperature, HMImTFSI is crystalline with $TFSI^-$ adopting the trans conformation. Upon melting, the spectra indicate the existence of both conformations (cis and trans) while at elevated temperatures cis conformation becomes dominant. The enthalpy of equilibrium between the two rotamers is, also, calculated from the reduced isotropic Raman spectra using the wagging SO_2 vibrations in 380–450 cm^{-1} region, and it was found ~8.5 kJ/mol.

1. Introduction

The low temperature relatives of molten salts, ionic liquids (ILs – liquids comprised of organic cations and organic/inorganic anions that melt at/or below 100 °C) [1] represent a class of materials with interesting properties such as low vapor pressure chemical stability, high conductivity, and low flammability [2,3]. ILs are often considered as "green" alternatives to organic volatile solvents, and as a result ILs have a wide range of possible applications in catalysis and biocatalysis [4–12] in electrochemistry [13–15], in materials synthesis [16,17], in chemical analysis [18–22], etc. However, studies on their toxicity [23], biodegradation [24], and chemical stability [25] as well as on the impact of the procedures used for their synthesis and purification [26] indicate that their characterization as "green" should differ not only with each IL but also with the intended use [25]. Thus to evaluate the environmental impact of each IL it is necessary to use suitable procedures and methodologies [27] (e.g. Life Cycle Analysis combined with economic optimization [28]).

Due to the great variety of anions and cations that can be combined, it is possible to prepare an almost unlimited number of ILs. Thus, it is of great importance to understand how their macroscopic properties (i.e. melting point, viscosity, conductivity etc.) depend on their structural properties. The understanding of these fundamental issues will be very helpful in order to design the appropriate IL for a given application. A great variety of studies using different techniques have been published concerning the impact of the structure on the properties of ionic liquids. At the molecular level, physicochemical properties depend on the interplay between Coulombic, van der Waals and hydrogen bond HB forces. For example, studies in imidazolium based aprotic ILs (AILs) using a variety of techniques (i.e. MD simulations [29–34], low frequency Raman [35,36], Optical Kerr Effect [37–39], NMR spectroscopy and X-ray and neutron diffraction [40,41]) have shown that the increase of the side chain of the cation results to a heterogeneity in the nanoscale regime by the formation of aggregates due to the competition between the electrostatic interaction of imidazole ring and anion with the collective short range interaction of the neutral alkyl chains [42–45].

Moreover, the degree of hydrogen bonding plays significant role on their properties. In order to explain the increased viscosity due

* Corresponding authors.
E-mail addresses: natassamoschovi@iceht.forth.gr (A.M. Moschovi), dais@iceht.forth.gr (S. Ntais), indy@iceht.forth.gr (V. Dracopoulos), vnikolak@iceht.forth.gr, vlad@udel.edu (V. Nikolakis).
[1] Present address: Institut National de la Recherche Scientifique, Énergie, Matériaux et Télécommunications (INRS-EMT), Université du Québec, Varennes, Canada.
[2] Present address: Catalysis Center for Energy Innovation, University of Delaware, DE, USA.

0924-2031/$ – see front matter © 2012 Elsevier B.V. All rights reserved.
http://dx.doi.org/10.1016/j.vibspec.2012.08.006

to the methylation of the $C_{(2)}$ position of C_4C_1ImCl, Hunt introduced the "entropy theory" [46]. According to their suggestion, the loss of hydrogen bonding due to methylation at $C_{(2)}$ position is outweighed by those due to entropy loss which in turn leads to an increase ordering in the liquid and thus higher melting points and viscosities are observed. Ludwig and co-workers [47] showed that the methylation in the $C_{(2)}$ position of the imidazolium ring increases the Coulombic interactions and this has an impact on the viscosity and the melting points. Recently, Noack et al. [48] concluded that both theories are complementary and a possible change of the electron density of the imidazole ring changes the position and the strength of interionic interactions and thus reduces the configurational variation that in turn affects the macroscopic properties. All the above reveals, that hydrogen bonding in ILs and the comprehension of its nature is very important [44].

Up to date, most of the studies concerning the structure of ILs have focused on AILs. However, another subset of ILs is the protic ionic liquids (PILs) which are formed through proton transfer from a Brønsted acid to a Brønsted base. Recently, two publications reviewed the physicochemical and thermal properties of PILs [1,49] highlighting their possible use in fuel cells, organic synthesis, in chromatography, as industrial lubricants, etc. One important difference between AILs and PILs is that in many cases the latter might vaporize even at relatively low temperatures as separate neutral Brønsted acid and base [50]. Angell and co-workers also showed that the excess boiling point of PILs depends on the difference between the pK_a values of the acid and base as determined in dilute aqueous solutions [51].

PILs are considered as promising candidate electrolyte materials for proton transfer in fuel cells and the understanding of their properties will have possibly a key role for the conceptual design and synthesis of PILs with improved properties for this purpose. Proton transfer in the case of PILs is described either by the Grotthuss type mechanism or by the vehicle type mechanism. In the latter, protons migrate attached to bigger carrier molecules (i.e. H_3O^+, HMI^+, etc.) which are called "vehicles". As a result, conductivity is determined by the molecular diffusion of the "vehicle(s)", which in the case of PILs are both ions. In the case of Grotthuss mechanism, protons are transferred from one "vehicle" to the next one, a movement known also as hopping. However, in order to create a percolating path for proton transfer, a reorientation–reorganization of the proton carriers is frequently required. Thus, we can say that in the case of the Grotthuss mechanism, conductivity depends on the proton transfer and on the proton carrier re-orientation rates [52]. The existence, the strength, and the directionality of hydrogen bonds between the different constituents of a PIL are expected to play a significant role in proton transfer by this mechanism. Hydrogen bonds are expected to enhance the ability of proton transfer between proton acceptors and proton donors as well as to restrict the reorientation ability of each ion. Furthermore, the formation of hydrogen bonded extended networks between ions that consist of multiple proton donor and acceptor centers, instead of hydrogen bonds that result in the formation of "ion pairs", are also expected to significantly affect the proton transfer rate. Only few studies have appeared in the literature investigating the proton transfer mechanism in the case of PILs. Watanabe and co-workers [45,53] studied extensively Brønsted acid–base binary mixtures using NMR and conductivity measurements. They have shown that the mechanism that governs the proton transfer depends on the imidazole content of the binary system. Far-IR [54] studies in both protic and aprotic ILs have shown that HB plays a more significant role in the case of PILs. Theoretical studies have also shown that in monomethylammonium nitrate (MMAN) PIL ion pairs are formed [55]. Also, very recently Martinelli et al. [56] discussed the conformational isomerism of the $TFSI^-$. Small and wide angle X-ray scattering studies showed that the change of the alkyl chain in alkylammonium based PILs follow the systematic that observed in aprotic ILs [41,57–60].

In the present work we focused on the PIL 1-H-3-methylimidazolium bis(trifluoromethanesulfonyl)imide (HMImTFSI) (see Fig. 1) in an attempt to understand the effect of temperature on the anion conformation. To achieve this, Raman and FTIR/ATR spectra were collected and analyzed at RT and up to 150 °C. Since, the melting point of HMImTFSI is within this temperature range, it is possible to record vibrational changes that occur upon melting.

2. Experimental

2.1. Sample preparation

1-H-3-methylimidazolium bis(trifluoromethanesulfonyl)imide (HMImTFSI) 99.5% (Fig. 1) was supplied in powder form by SOLVIONIC S.A. Liquid methylimidazole (MIm) > 99% was purchased from Sigma–Aldrich Co. All chemicals were stored and manipulated in a glove bag under Ar atmosphere at room temperature and used without further purification.

2.2. DSC measurements

Differential scanning calorimetry was carried out in order to determine the melting point of the ionic liquid HMImTFSI. Measurements were obtained using a TA Q100 Differential Scanning Calorimeter. The sample was sealed hermetically in plain aluminum pans and it was heated from −100 °C up to 400 °C with heating rate 5 °C/min.

2.3. FT-Raman measurements

FT-Raman spectra were obtained at room temperature and at 60, 90, 120 and 150 °C, using a Bruker (D) FRA-106/S component attached to an EQUINOX 55 spectrometer. An R510 diode pumped Nd:YAG laser at 1064 nm operating at 250 mW was used for Raman excitation. Initially, samples were introduced into quartz tubes (OD: 6/ID: 4), dried and sealed under vacuum in a homemade glassy vacuum line. The spectra were recorded using a 4 cm^{-1} resolution and 100 scans.

For the spectra of the liquids (temperature range: 60–150 °C) two different polarization configurations were used: the vertical–vertical (VV) and the vertical–horizontal (VH). Before starting any experiment in the FT-Raman system, a calibration of the depolarization ratio was made by recording the spectra of CCl_4.

For measuring at temperatures above 25 °C, a home-made optical furnace was designed and constructed. The furnace was built up using a resistance sandwiched between two metallic bronze plates. This block was further inserted in a Teflon cover in order to avoid thermal leakage. The temperature was controlled with a K-type thermocouple (RS Components Ltd.) at the back of the cell through a microcontroller (CAL Controls Ltd., Model cal3300). In order to ensure that there is no deviation between set temperature and sample's temperature, another K-type thermocouple (RS Components Ltd.) was placed just above the scattering area.

2.4. FTIR/ATR measurements

FTIR/ATR spectra were collected at the same temperature range as in Raman spectroscopy, using a Bruker Equinox 55 spectrometer, equipped with a single reflection diamond ATR attachment (Model: MKII Golden Gate, SPECAC Ltd.) which can operate at temperature up to 200 °C. The ATR attachment had KRS-5 lenses, enabling the acquisition of spectra from 400 cm^{-1}. For room temperature measurements sample was placed on diamond crystal and compressed

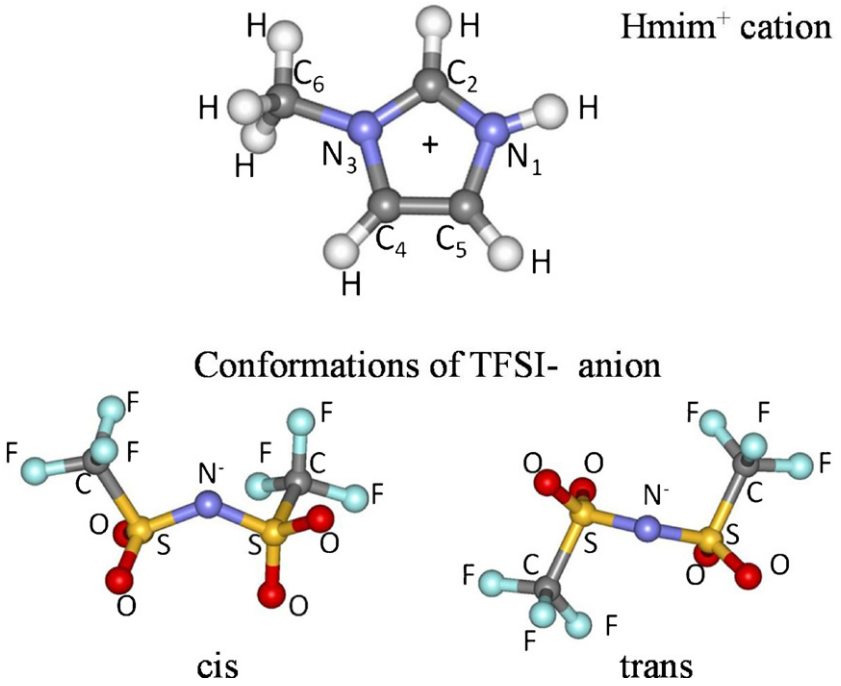

Fig. 1. Schematic of the 1-H-3-methylimidazolium cation and the two conformers (cis, trans) of the $TFSI^-$. Atom numbering in cation scheme is used in the discussion.

using the anvil of the ATR attachment. For temperatures higher than melting points, the anvil was removed and the diamond surface was entirely covered with a thin film of HMImTFSI. Spectra were recorded at 4 cm^{-1} resolution with 50 scans under N_2 atmosphere. It is very important to note here that, a background spectrum at each measuring temperature was collected before recording the FTIR/ATR spectra of the sample.

The FT-Raman and FTIR/ATR spectra were collected more than once to ensure reproducibility and only a portion of them is presented here. Above 100 °C the high wavenumber region of the Raman spectra was not analyzed because it is dominated by a broad band due to blackbody radiation.

3. Results and discussion

HMImTFSI is a crystalline solid at room temperature. Its melting point, as determined from DSC measurements, is ~52 °C (see supporting info, Fig. SI-1). This value is in agreement with that recently reported by Peppel et al. [61] indicating that the commercial PIL sample was of equal purity. Tables 1 and 2 present all the observed bands of the Raman and FTIR spectra of the solid and liquid phase, respectively. The spectral regions that are not analyzed in the present text are presented in the supporting info (Figs. SI-2 and SI-3).

3.1. Effect of melting on $TFSI^-$ conformation

HMImTFSI crystallizes in P2-1/c monoclinic space group [61] having two anions and two cations in the unit cell. Hydrogen bonding between the anion and cation takes place through the N—H and $C_{(i)}$—H (*i*: 2, 4, 5 position) groups of $HMIm^+$ and the oxygen atoms of $TFSI^-$. Thus, it is expected that the spectral changes related with the SO_2 vibrational modes can give information concerning the conformational isomerism of the $TFSI^-$. Upon melting, no significant changes were observed in the FTIR and Raman spectra of the symmetric and antisymmetric modes of SO_2 at ~1130 cm^{-1} and ~1350 cm^{-1} (see Figs. SI-4 and SI-5). Thus, our discussion is focused in the bending, twisting, wagging and rocking modes of SO_2. These vibrations are observed in the Raman spectra between 250 and 450 cm^{-1} and the FTIR spectra between 400 and 700 cm^{-1} (Figs. 2 and 3).

The Raman spectra of the solid (Fig. 2) is dominated by the vibrational modes of the $TFSI^-$ [56–58,62,69] since $HMIm^+$ has little or no contributions, as it can been seen from FT-Raman spectrum of MIm (Fig. SI-6). The bands at 277, 299, 315, 340, 402 and 412 cm^{-1} are associated to the trans conformer while the one at 356 cm^{-1} could arise from both the trans $TFSI^-$ and $HMIm^+$ [62–67].

Upon melting several changes are observed. The low wavenumber band at 277 cm^{-1}, shifts slightly to higher frequencies, while the bands at 299, 315, 340 and 356 cm^{-1} become broader. Moreover, the band at 299 cm^{-1}, which is well defined in the spectra of the solid, almost disappears under the envelope of the 279 cm^{-1}

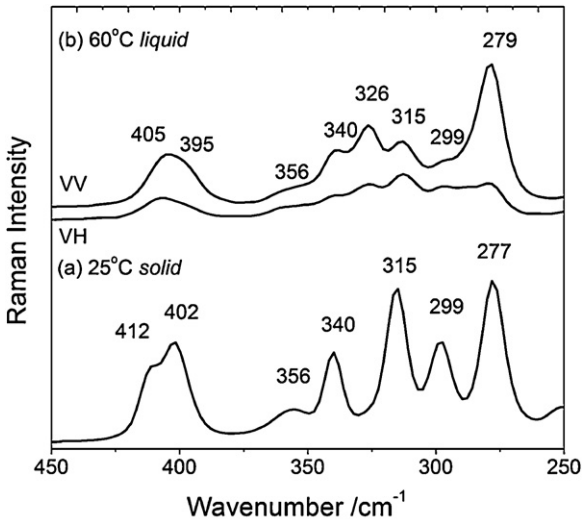

Fig. 2. FT-Raman spectra of the HMImTFSI between 450 and 250 cm^{-1} of the (a) solid at 25 °C and (b) the liquid at 60 °C in VV and VH polarization configurations.

Table 1
Observed Raman bands of HMImTFSI at different temperatures and their assignment according to the literature (the spectra are shown in Fig. SI-2).

$\theta = 25\,^{\circ}C$, ω (cm^{-1})	$\theta = 60\,^{\circ}C$, ω (cm^{-1})	$\theta = 90\,^{\circ}C$, ω (cm^{-1})	$\theta = 120\,^{\circ}C$, ω (cm^{-1})	$\theta = 150\,^{\circ}C$, ω (cm^{-1})	Assignment	Refs.
186w[a]	172 (p)[c]w[d]	170	170	171		
211vw	211 (dp)vw	211[h]			γNCH_3[e,f]	[69]
250w	244(dp),vw	242	240	240		
277s	279(p),s	278	279	278	ρCF_3	[66,84]
299m	(294)[b] (dp),vw	(296)			ρCF_3, $\nu_{as}CS$	[56,62,84]
315w	313(dp),m	313	312	313	ρSO_2, ρCF_3, $\nu_a CS$	[56,62,66]
	326(p),ms	326	326	325	ρSO_2	[56,66,82]
340m	339(dp),m	338	(337)	(337)	τSO_2	[56,66,82]
356vw	(356)(dp),w	(354)	(354)	(351)	τSO_2, δNCH_3	[56,66,69]
402m	(395)(p),m	(397)	(396)	(395)	ωSO_2	[62,66]
	405(p),m	404	404	404	ωSO_2	[63,66]
412m					ωSO_2	[63,66]
514					$\delta_a CF_3$	[66]
537w					$\delta_s S—C$	[84]
552w	552(dp),w	552	552	552	$\delta_s SO_2$	[66]
559w	(557)(dp)	(557)	(557)	(557)		
570m	570(p),w	570	570	570	$\delta_a CF_3$, $\delta^{ip}{}_s R$	[66,67]
590w	589(p),w	589	589	589	$\delta_a CF_3$, $\delta_a{}^{ip}SO_2$, $\delta_s NSO_2$	[62,66]
624vw	622(dp),vw	623	623	621	γ(R), δSNS	[69,62]
632vw					$\delta_s CF_3$, $\delta_s N—SO_2$	[62]
665ms	663(p),ms	663	663	662	δSNS, $\nu N—CH_3$	[66,69]
745vs	741(p),vs	741	740	740	$\delta_s CF_3$	[56,66]
796w	795(dp),vw	796	795	794		
917w	916(dp),w	916	916	916	γCH	[69]
1007ms	1010(p),m	1010	1010	1010	δ(R)	[69]
1087ms	1087(p),ms	1089	1088	1088	δCH, δCH + ν(R)	[69,82]
1100m	(1100)(dp)	(1105)	(1105)	(1107)	$\nu^{ip}{}_s R$, $\nu C—C$, $\delta_s HC—CH$, $\rho^{op}CH_3$	[67,69,82]
1133ms	1133(p),ms	1134	1133	1132	$\nu_s SO_2$	[62,66]
(1142)[b]					$\nu_s SO_2$	[66,67]
1163vw	1160(dp),vw	1165				
1183vw						
1244s	1240(p),s	1241	1240	1239	$\nu_s CF_3$	[62,66,84]
1280w	1280(p),m	1282	1280	1280	δCH	[69]
1305m	1308(p),m	1309	1309	1308	CN ring	[69]
1332m	1332(dp),m	1331	1330	1330	$\nu_{as}SO_2$, δCH_3, ν(R)	[62,64,66,69]
1352m	(1367)(p)	(1369)	(1369)	(1365)	ν(R)	[69]
1383m	1383(p),m	1382	1382	1383	ν(R)	[69]
(1424)					$\delta_s(CH_3)$	[69]
(1432)					$\nu_a{}^{ip}R$, $\nu C—C$, $\nu CH_3—N—CN$	[67]
1444s	1447(p),s	1446	1446	1445	δCH_3	[69]
1473vw	(1475)(dp)	(1476)	(1471)		δCH_3	[69]
1549w	1553(p),w	1552	1551	1550	ν(R)	[69]
1584w	1587(p),w	1586	1585	1586	ν(R)-MIm$^+$	This work
2835m	2836(p),m	2836	2836	*[g]	ν(R) + δCH_3	[69,82]
(2941)vw	(2941)(p)	(2943)	(2933)	*		
2967m	2969(p)ms	2969	2969	*	$\nu_s CH_3$	[69]
2980w						
3020w	3020(p),w,br	3016	3014	*		
3037w	3041(dp),vw	3038	3035	*		
3084w	3086(p)vw	3086	3085	*		
3141m	3145(p),w	3146	3147	*	$\nu C_{(2)}—H$, $\nu C_{(i)}—H$	[69,82]
3151w						
3185w	3189(p),w	3188	3187	*	$\nu C_{(4,5)}—H$	[69]
3287w	3281(dp),vw,vbr	3277	*	*	ν-NHO	[76,77]

[a] Frequencies with an estimated error ±1 cm^{-1}.
[b] Numbers in parentheses indicate shoulder bands with an estimated error ±5 cm^{-1}.
[c] The symbol in parentheses indicate the polarization state of each band; p: polarized, dp: depolarized.
[d] Letters indicate the relative intensities of the observed bands; vw: very weak, w: weak, m: medium, ms: medium strong, s: strong, vs: very strong, br: broad and vbr: very broad.
[e] Letter before the characteristic group, stands for the vibration type: ν: stretching, δ: in plane bending, τ: twisting, ρ: rocking, γ: out of plane bending, w: wagging.
[f] ip: in phase, op: out of phase, s: symmetric, as: asymmetric.
[g] Asterisk denotes that the bands are not observable due to blackbody radiation.
[h] Spectral characteristics are similar to that noted for 60 °C and thus no further notation is given.

band in the spectra of the liquid. At the same time a new polarized band at 326 cm^{-1} appears, while the SO_2 modes wagging at 395–415 cm^{-1} spectral region, exhibit a red shift with a concomitant inversion on their intensities. The later spectral characteristics have also been observed in other $TFSI^-$ containing ionic liquids and were attributed to the cis conformer [63].

The corresponding FTIR/ATR spectra are shown in Fig. 3. The presence of a characteristic band of the trans conformer (~607 cm^{-1}) in the spectra of the solid, indicates that this is the dominant conformation of $TFSI^-$. The spectra of the liquid however, exhibit the characteristic bands at 600 and 653 cm^{-1}, which are correlated to the cis conformer.

In conclusion our results strongly imply that the $TFSI^-$ is in the trans conformation in the crystalline phase, while upon melting the cis and the trans conformers coexist.

As mentioned above the unit cell of HMImTFSI crystal has two anions and two cations. Four hydrogen bonds are formed between the $N_{(1)}—H$, $C_{(2)}—H$, $C_{(4)}—H$ and $C_{(5)}—H$ and the oxygen atoms of

Table 2
Observed FTIR/ATR bands of HMImTFSI at different temperatures and their assignment according to the literature (the spectra are shown in Fig. SI-3).

θ = 25 °C, ω (cm^{-1})	θ = 60 °C, ω (cm^{-1})	θ = 90 °C, ω (cm^{-1})	θ = 120 °C, ω (cm^{-1})	θ = 150 °C, ω (cm^{-1})	Assignment	Refs.
(507)[b]w	509[a]m	509	508	508	$\delta_a CF_3$[d,e]	[66]
514m	516w[c]	515[f]	515	515	$\delta_a CF_3$	[66]
540vw						
553vw						
570m	569m	569	569	569	$\delta_a CF_3$, δ_aR	[66,67]
(599)m	600m	600	600	600	$\delta_a{}^{ip}SO_2$, CH_3N, $\delta^{ip}{}_sR$	[66,67]
607m	610m	610	610	610	$\delta^{op}{}_aR$, δSNS, $\delta_a{}^{op}SO_2$	[62,66,67]
630w	(623)w	(623)	(623)	(623)	$\delta^{op}{}_{as}R$	[63]
	653vw	653	653	653	δ_aR, δSNS, CH_3NCN	[66,67,83]
	(664)vw	(664)	(664)	(664)	ν(R)	
743w	740w	740	739	739	$\delta_s CF_3$, δR, CH_3N, $\delta^{ip}R$, δ_sR,HC—CH	[66,67,83]
	752vw	(752)	(751)	(751)	δ_sHCCH	[67]
766m	763vw	762	(762)	(763)	ν_sSNS, δ_aHCCH	[66,67]
792m	790vw	789	789	788	νCS, δ_aHCCH	[62,66,67]
861vw	855vw	855	853	850	ν_aSNS	[66]
917vw	916vw	915	915	915	ν(R)	
(1004)w	1011vw	(1011)	(1011)	(1014)	δ(CH)	
1039s	1041s	(1037)	(1037)	(1038)	ν_sR, CH_3N, νCH_2N, νSO, $\nu_s{}^{ip}R$	[67,83]
1051s	1051s	1051	1051	1051	ν_aR, νCC, $tNCH_3$, ν_aSNS	[62,66,67]
1086m	1087w	(1083)	(1083)	(1083)	νCC, ν_sR, δCH	[67,82]
1099m	1106(sh)w	1105	1105	1106	δCH	[82]
1128s	1129s	1130	1129	1129	$\delta_s{}^{ip}SO_2$, ν_sSO_2	[66,67,80,83]
(1165)s					$\nu_a{}^{ip}R$, νC—C, N—CH_3	[67,83]
1180s	1179vs	1179	1179	1179	ν_sR, νN—CH_3, ν_aCF_3, νN—CH_3CN	[67,83]
1219m					ν_sCF_3	[66,67]
(1226)m	(1225)m	1223	(1222)	(1222)	ν_aCF_3, νCN	[66,67,82]
(1240)w	(1242)vw	(1240)	(1236)		ν_sCF_3	[66]
1280vw	1283vw	1283	1283	1281	$\nu_a{}^{ip}R$, νC—C, νCH_3NCN	[83]
1305ms	(1308)ms	(1312)	(1312)	(1311)	ν_sCF_3	[66]
1328s	1327m	1328	1328	1328	$\nu_a{}^{op}SO_2$, ν_sR, νCC, νCH_3NCN	[62,66,67,80]
1349s	1345ms	1346	1346	1344	$\nu_a{}^{ip}SO_2$,	[62,66,67,80]
1430vw	(1431)vw	(1428)vw	(1430)	(1430)	δ_sCH_3, ν^{ip}aR	[67,69,82]
1445 vw	1447w	1447w	1445	1475	δ_aCH_3	[82]
1456 vw	(1454)vw				δ_aCH_3	[82]
1473 vw	1475vw				$\nu^{ip}{}_a$,δ_aCH_3, νCH_3	[67,69]
1548w	1553vw	1553	1552	1552	ν(R)	
1584w	1588vw	1589	1587	1586	$\nu^{ip}{}_{s/a}$R, νCH_3, $\nu_s{}^{ip}R$, νCH_3N, $\nu^{ip}R$	[67,82]
2985m,vbr					ν_sCH_3	[67,82]
3080m	3087vw	3087	3087	(3088)	νC_2H	[45,68,81]
3115ms	3122vw	3124	3124	(3122)	νC_2H	[45,67,68,83]
3140m						
3150s						
3163m	3163v	3166	3165	3165	$\nu C_{4,5}H$	[45,83]
3192w						
3271vs	3273vw,vbr	3274	3275	3277	ν-NHO	[66,76,77]

[a] Frequencies with an estimated error ±1 cm^{-1}.
[b] Numbers in parentheses indicate shoulder bands with an estimated error ±5 cm^{-1}.
[c] Letters indicate the relative intensities of the observed bands; vw: very weak, w: weak, m: medium, ms: medium strong, s: strong, vs: very strong, br: broad and vbr: very broad.
[d] Letter before the characteristic group, stands for the vibration type: ν:stretching, δ:bending, τ: twisting, ρ: rocking, w: wagging.
[e] ip: in phase, op: out of phase, s: symmetric, as: asymmetric.
[f] Spectral characteristics are similar to that noted for 60 °C and thus no further notation is given.

$TFSI^-$. The two of them between the N—H group and the two oxygen atoms of the same anion are referred as those of the higher strength. The latter was attributed to the "pre-formation" of ion pairs [61]. Our observation of the cis conformer in the liquid phase can be considered as an indication of the formation of ion pairs since the oxygen atoms of both O=S=O groups of the anion are facing in the same direction and thus it is easier to form strong HBs with the same cation, instead of a hydrogen bond network. Due to the absence of any solvent in our system we use the term ion-pair to denote the formation of strong HBs only between anion and cation pairs.

3.2. Effect of melting on NH and CH stretching vibrations

The existence of hydrogen bonds is expected to affect also the N—H and C—H vibrational modes. The high frequency area at 2750–3450 cm^{-1} (Figs. 4 and 5), which is correlated to the vibrations of the cation can give information concerning the changes of the aforementioned groups. Bands detected below 3000 cm^{-1} are attributed to methyl and/or alkyl groups symmetrical stretching vibrations [78] while the bands observed between 3000 and 3200 cm^{-1} are due to the $C_{(i)}$—H stretching modes. Moreover, the more acidic $C_{(2)}$—H vibrations are expected at lower wavenumbers than those of the $C_{(4,5)}$—H vibrations [68,69]. Bands at higher wavenumbers, which are attributed to N—H modes, are also detected in Figs. 4 and 5 of FT-Raman and FTIR/ATR spectra, respectively. It must be mentioned however, that the hydrogen bonded N—H···O, as expected, exhibit weak and broad Raman bands. On the other hand, the same vibrations exhibit a more intense band in IR spectra.

Bands in this region are also reported in similar studies. In the IR spectra of the gas phase of HTFSI Rey et al. [66] found a band at 3394 cm^{-1} and Foropoulos and DesMarteau [70] found two bands at 3395 and 3220 cm^{-1}. The second band was assigned to the N—H stretching vibration of the HTFSI in the gas phase. Furthermore, in

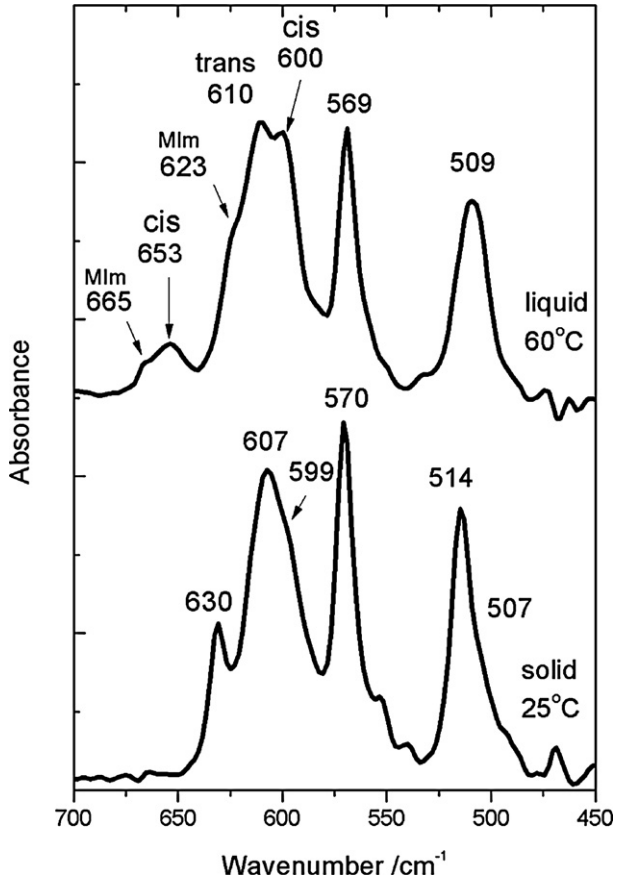

Fig. 3. FT-IR/ATR spectra of the HMImTFSI between 700 and 450 cm^{-1} of the solid at 25 °C and the liquid at 60 °C.

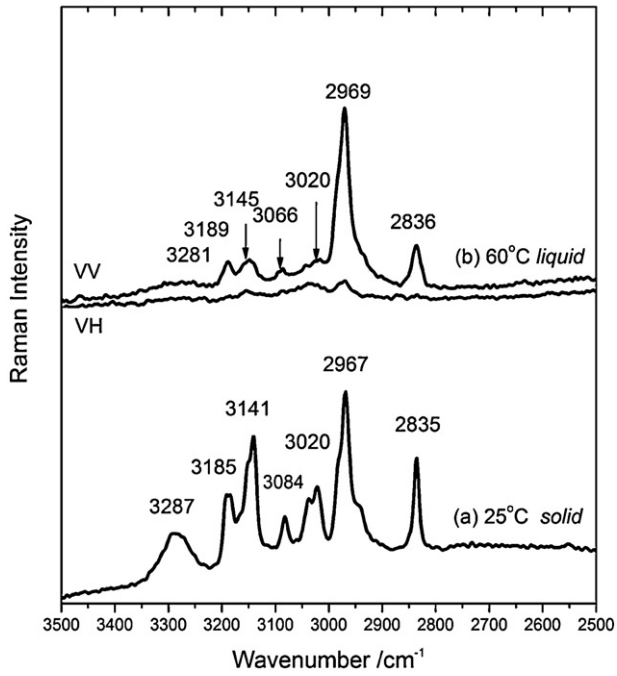

Fig. 4. FT-Raman spectra of the HMImTFSI between 3500 and 2500 cm^{-1} of the (a) solid at 25 °C and (b) the liquid at 60 °C in VV and VH polarization configurations.

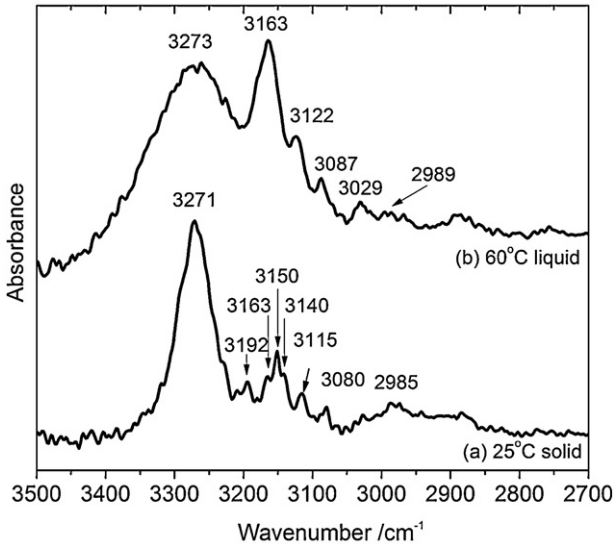

Fig. 5. FTIR/ATR spectra of the HMImTFSI between 3500 and 2700 cm^{-1} of the (a) solid at 25 °C and the (b) liquid at 60 °C.

the FTIR spectra of the polybenzimidazole (PBI)/sulfonated polysulfone (SPSF) blends [71] a band around ~3400 cm^{-1} was attributed to the free N—H stretching modes while a broad band detected at 3145 cm^{-1} to the H-bonded self-associated N—H species. Similar results were reported also in the cases of other H-bonding polymers like nylon [72,73]. Consequently, the observed Raman band at 3287 cm^{-1} (Fig. 4) and the FTIR band at 3271 cm^{-1} (Fig. 5) of the solid HMImTFSI can be assigned to the N—H vibration of H-bonded N—H···O=S=O group. Upon melting the intensity of the Raman band significantly decreases while the FTIR band broadens.

A qualitative estimation of the strength of the hydrogen bond is the wavelength difference of the peaks attributed to the free and the H-bonded species [74–77]. There are no references concerning the position of the characteristic band of the hydrogen bond free N—H group. So in order to have a first approximation about the strength of the N—H···O hydrogen bond we compared the wavenumber of the band that is characteristic of H-bonded species with that of the free N—H of PBI/SPSF blends. This comparison is reasonable due to the imidazolium based structure of PBI. Thus, this wavelength difference is ~129 cm^{-1}, while in the PBI/SPSF systems is ~250 cm^{-1} [68]. This result denotes that the N—H···O HB in the HMImTFSI is of lower strength compared to that in PBI/SPSF systems.

Since upon melting the Raman band around 3287 cm^{-1} is not detected, our discussion will be focused to the corresponding FTIR band. The ratio of the area of the N—H FTIR band to the total area of the bands that are assigned to stretching vibrational modes of the $C_{(i)}$—H and N—H···O remain constant in both solid and liquid spectra, so we can assume that their population does not change remarkably in the melt and that the average enthalpy of the N—H···O hydrogen bonds is not affected by melting. The broadening upon melting can be attributed to the change of the anion's conformation. More specifically, in the crystal the local HB geometries between the N—H groups of the imidazolium ring and the oxygen atoms of the SO_2 groups are more oriented and well defined since only one conformer exists. Upon melting however, the existence of both cis and trans conformers alters this directionality of the N—H···O bond affecting the FWHM of the band at 3271 cm^{-1}.

The Raman and FTIR bands between 2800 and 3200 cm^{-1} undergo a blue shift upon melting indicating that hydrogen-bonds through the $C_{(i)}$—H groups are weaker in the liquid. The FTIR bands at 3150 and 3315 cm^{-1} shift to 3163 and 3122 cm^{-1}, respectively, while the Raman bands at 3185 and 3141 cm^{-1} are detected at

3189 cm^{-1} and 3145 cm^{-1}. In both spectra the high frequency modes are correlated with the $C_{(4,5)}$—H symmetric stretching modes while the low frequency to the $C_{(2)}$—H symmetric stretching vibrational mode.

The $C_{(i)}$—H (*i*: 2, 4, 5) vibrational modes in Raman spectra are at higher frequencies than those of PF_6^- or Cl^- based imidazolium ILs [78]. The $C_{(2)}$—H symmetric stretching shifts from 3062 to 3115 to 3145 cm^{-1} and the $C_{(4,5)}$—H shifts from 3142 to 3180 to 3189 cm^{-1} (for Cl^-, PF_6^- and $TFSI^-$, respectively). The higher shift observed in the $C_{(2)}$—H symmetric stretching indicates that the hydrogen bonds through this position are affected more than those through the $C_{(4,5)}$—H. This is consistent with the expected weakening of the HBs in these liquids. Even though the cation around PF_6^- or Cl^- is different and these ionic liquids are aprotic the trend is clear. Moreover, the decrease of the intensity of the $C_{(2)}$—H modes upon melting is an indication that the population of these bonds may be affected from the melt structure.

Based on the above, we propose that the liquid structure of HMImTFSI is formed by ion pairs connected primarily with N—H···O bonds the strength of which is widely distributed due to coexistence of the two conformers of $TFSI^-$ in the liquid. In any case, discussion about H-bonding must be taken with care. Further studies with X-ray and/or neutron scattering techniques as well as theoretical calculations are necessary to provide further insight in understanding the structure of the protic ionic liquid HMImTFSI.

3.3. Temperature effects on the spectra of the liquid

In the previous section, we showed that the $TFSI^-$ can change its conformation from cis to trans and vice versa depending on temperature. Vibrational spectroscopy is one of the most powerful techniques for providing quantitative information on such conformational changes. Raman scattering as well as IR absorption techniques have been widely used to investigate these changes over the last few years [56,63,66]. The main conclusion from these studies is that the trans conformer is more stable at low temperatures while the cis one is favored at higher temperatures. A long-standing concern in the current literature is related to the selection of the proper spectral area to be used for the cis–trans equilibrium determination. The number of individual vibrational lines employed in the fitting analysis is also a point of controversy. However, the spectral range 250–450 cm^{-1} in the Raman spectra is considered as the best choice because (i) there is a little influence from bands related to the cation motion and (ii) the Raman lines corresponding to the two conformers can be separated with enough accuracy.

A major shortcoming of the previous investigations is the lack of a certain protocol for the quantitative determination of the cis-trans equilibrium. The polarization geometry of the Raman scattering experiment is seldom mentioned. Further, several different laser lines have been used, while no correction for the temperature effect on Raman scattering intensity is taken into account. In the next paragraphs, we will briefly refer to the correction steps needed to be done to the experimental Raman intensity in order to achieve a reliable estimation of the cis–trans equilibrium.

In a routine Raman scattering experiment all the Raman active modes of a molecule can be obtained by measuring polarized and depolarized spectra. The most common polarization geometries for isotropic media (e.g. liquids) are those denoted as VV (where the electric vector of the incident and the scattering radiation is vertical to the scattering plane) and VH (where the electric vector of the incident radiation is horizontal to the scattering plane and vertical that of the scattering radiation). By using these two scattering intensities the isotropic and anisotropic intensities at wavenumber (ω) can be calculated by using the following equations

$$I_{iso}(\omega) = I_{VV}(\omega) - \frac{4}{3} I_{VH}(\omega) \quad (A.1)$$

$$I_{aniso}(\omega) = I_{VH}(\omega) \quad (A.2)$$

The isotropic and anisotropic scattering spectra are used to separate the pure vibrational motion (isotropic part arising from the diagonal part of the polarizability tensor) of a molecule from its anisotropic part (re-oriententional motion and bond bending modes).

The quantitative analysis of Raman spectra necessitates the use of the so-called *reduced representation*. The reduction considers the distortion of the experimental Raman spectra that has taken place in view of the finite sample temperature and the wavelength dependence of the scattered light. Since the Raman scattering is a pure quantum mechanical effect the elementary vibrational transitions taking place during the process depend upon the population of the energy levels.

In general, the experimental scattered light intensity can be expressed as follows:

$$I_\sigma(\omega) = G_{exp}\omega(\omega_L \pm \omega)^{-4} M_\sigma B^{-1}(\omega) \quad (A.3)$$

where σ stands for VV, VH, ISO and ANISO, G_{exp} is a constant that correlated with the experimental set-up, M_σ is the integral function of the polarizabilty and $B(\omega,T)$ is a temperature function related to Boltzman population factor $n(\omega)$ which for the Stokes part of the Raman spectrum is given by

$$B(\omega, T) = n(\omega) + 1 \quad \text{where } n(\omega) = \left[\exp\left(\frac{h\omega}{kT}\right) - 1\right]^{-1} \quad (A.4)$$

The Boltzman factor accounts for the temperature contribution to the vibrational lines and thus it must be removed. The reduced spectrum $R_\sigma(\omega)$ is calculated from the $I_\sigma(\omega)$ by the following equation:

$$R_\sigma(\omega) = (\omega_L \pm \omega)^{-4} \omega B(\omega, T) I_\sigma(\omega) \quad (A.5)$$

where corrections for both the wavelength and the temperature dependence of the scattering are included. More detailed analysis and justification of the reduction procedure in the Raman spectra of glasses and liquids can be found elsewhere [79].

Following the correction steps mentioned above we propose that the reduced isotropic part of the Raman spectrum, R_{iso}, is the most appropriate part of the scattering intensity for analyzing thermodynamic properties, such as ΔH between species that are in equilibrium, since it considers the pure vibrational motion, disentangled also from any distortion due to thermal factor and/or wavelength. In Fig. 6 we present reduced isotropic Raman spectra over the 350–450 cm^{-1} spectral range for all measured temperatures. It is clear that there is a systematic behavior of the bands related with two conformers as the temperature changes. More specifically, with increasing temperature, the intensity of the bands that correspond to C_1 conformer increases in comparison to the intensity of the bands arising from the C_2 conformer. From the ratio of the integrated intensities of certain bands we can calculate the population ratio of the two conformers as follows:

$$\frac{I_{C_1}^{X_1}}{I_{C_2}^{X_2}} = \frac{C_1}{C_2} \quad (A.6)$$

where X_1 and X_2 state for the appropriate band frequencies used in the present calculation. The relative spectral changes of the two bands assigned to the cis/trans conformers in the melt indicate that these two are in equilibrium. The equilibrium constant K characterizing the cis ↔ trans transformation is related to changes of

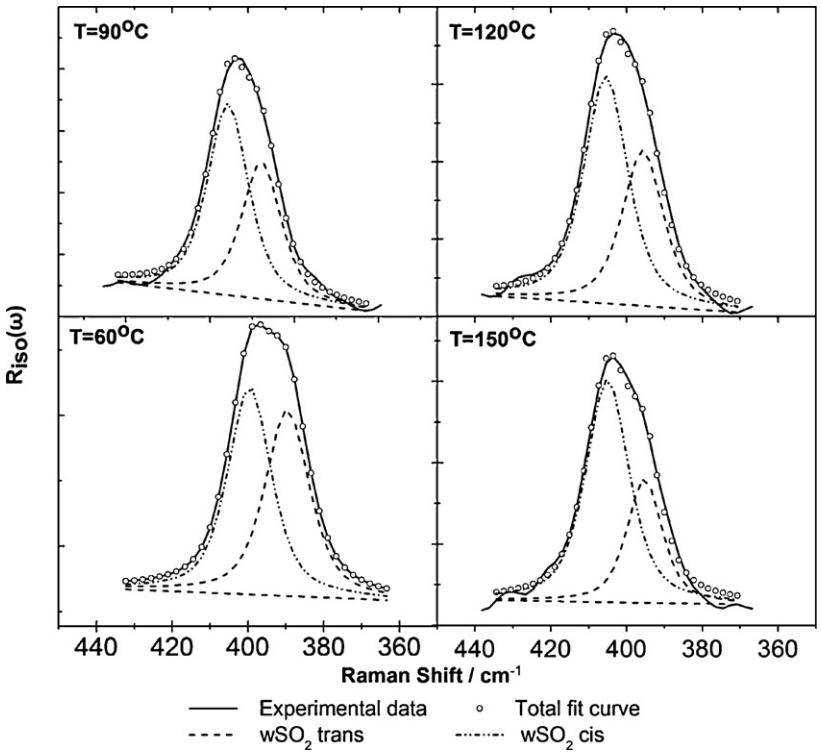

Fig. 6. Dencovoluted temperature dependence R_{iso} FT-Raman spectra of the liquid HMImTFSI at temperature range from 60 °C up to 150 °C in the 370–440 cm^{-1} range of SO_2 wagging mode. Thick solid line: experimental data, open circles: total fit curve.

basic thermodynamic functions like ΔH and ΔS and is given by the relation:

$$-RT\ \ln K = \Delta H - T\,\Delta S \tag{A.7}$$

where R is the gas constant and T is the absolute temperature. The constant K is defined as the ratio of the concentrations Y of the two conformers:

$$\frac{Y_{C_1}}{Y_{C_2}} = K \tag{A.8}$$

The concentration Y of each conformer in turn is related with the Raman scattering intensity through:

$$I_{C_i} = Y_{C_i} R_{C_i} \tag{A.9}$$

where R_{C_1} is the Raman scattering coefficient of the C_i (i: 1, 2) conformer. By substituting Eqs. (A.8) and (A.9) to Eq. (A.7) and dividing with −RT yields,

$$\ln \frac{I_{C_1}^{X_1}}{I_{C_2}^{X_2}} = -\frac{\Delta H}{RT} + \frac{\Delta S}{R} - \ln \frac{R_{C_1}}{R_{C_2}} \tag{A.10}$$

The use of the above relation is possible only when the Raman scattering coefficients of the conformers and their temperature dependence are known. In most cases, it is tacitly assumed that R_{C_1} are equal and temperature independent so they cancel out in Eq. (A.10). However, the above assumptions can be considered as good approximations for vibrational modes of common origin, i.e. when the modes are of the same symmetry (e.g. wagging modes of the two conformers). On the contrary, the equality of R_{C_i} for the two conformers is not in general a valid assumption for modes that arise from different types of vibration, i.e. when one compares a rocking and a wagging mode. In the present case we have chosen to compare the scattering intensities of the SO_2 wagging mode, with this species being in a cis and a trans conformation. The modulations of the atom polarizability during the S—O vibrations inside a cis and a trans conformer are of the same magnitude since it depends on the geometrical features of the bond configuration. Obviously, the local environment around a S=O bond is not appreciably different in cis and trans conformations. This proximity of the local geometrical features around an S=O bond in cis and trans species implies further a common temperature dependence of the polarizability modulation arising from the wagging type vibrational motion. Based on the aforementioned arguments, Eq. (A.10) can be re-written as:

$$\ln \frac{I_{C_1}^{X_1}}{I_{C_2}^{X_2}} = -\frac{\Delta H}{RT} + \frac{\Delta S}{R} \tag{A.11}$$

From the latter equation we can calculate the ΔH from the slope of the plot of $\ln(I_{C_1}/I_{C_2})$ vs. T^{-1}.

The vibrational modes that are used for this calculation are the SO_2 wagging modes at 397 cm^{-1} (for C_2 conformer) and 405 cm^{-1} (for C_1 conformer) as estimated after the deconvolution of the broad band centered at ~400 cm^{-1}. For the deconvolution we use a combination of Lorentz and Gauss functions with a certain relative ratio as proposed elsewhere [80] which was kept constant for both bands of the two conformers at all temperatures. The same fitting procedure was followed also for the deconvolution of the corresponding peaks in the isotropic spectra. A van't Hoff plot of the values obtained from both R_{iso} and I_{iso} spectra is shown in Fig. 7. The plotted values follow Eq. (A.11). This is in agreement with the previous studies in $TFSI^-$ containing liquids, showing that the trans conformer is also in our case more stable at lower temperatures. Apart from the fitting procedure it is evident that there are significant differences in the calculated values of ΔH as the temperature factor in the vibrational spectra is corrected, which in turn proves the proposed procedure. Even though our calculation cannot be compared directly with the literature measurements (Table 3) the finding value of ΔH = 8.5 (±0.6) kJ/mol is comparable to that of other $TFSI^-$ containing liquid systems (Table 3).

Table 3
ΔH of conformational isomerism of the $TFSI^-$ in imidazolium based ILs.

Cation of ionic liquid	Method	Laser line (nm)	Polarization	Reduced spectra	cis[a]	trans[b]	ΔH (kJ/mol)	Refs.
Tetraethylammonium								
Et_4N^+	Raman	514.5	N/A	–	321, 326 (ρSO_2)	340 (τSO_2)	8 ± 1	[80]
1-Ethyl-imidazolium								
EIm^+	Raman	514.5	N/A	–	306, 326, 333 (ρSO_2)	298(ρCF_3), 314, 339(τSO_2)	3.38 ± 0.22	[56]
EIm^+	Raman	514.5	N/A	–	739($\delta_s CF_3$)	742($\delta_s CF_3$)	4.95 ± 0.81	[56]
1,2-Dimethyl-3-N-ropylimidazolium								
$DMPIm^+$	Raman	514.5	N/A	–	306, 326, 333 (ρSO_2)	298(ρCF_3), 314, 339(τSO_2)	4.88 ± 0.6	[56]
$DMPIm^+$	Raman	514.5	N/A	–	739($\delta_s CF_3$)	742($\delta_s CF_3$)	4.32 ± 0.7	[56]
1-Methyl-pyrrolidinium								
MPD^+	Raman	514	N/A	–	306, 326, 333	298, 314, 339	6.19 ± 0.23	[56]
MPD^+	Raman	514	N/A	–	739($\delta_s CF_3$)	742($\delta_s CF_3$)	7.28 ± 275	[56]
1-Ethyl-3methyl-imidazolium								
$EMIm^+$	Raman	1064	N/A	–	407($_\omega SO_2$)	398($_\omega SO_2$)	3.5 ± 0.1	[64]
Lithium								
LiTFSI Solution in glymes	FTIR	–	–	–	656, 602($\delta^{ip}{}_a SO_2$)	618($\delta^{op}{}_a SO_2$)	2.2 ± 0.5	[62]
1-H-3-methyl-imidazolium								
Him^+	Raman	1064	*A*	R^{iso}	406	396	8.5 ± 0.6	This work

[a] Vibrational modes used as indicators for cis conformation.
[b] Vibrational modes used as indicators for trans conformation.

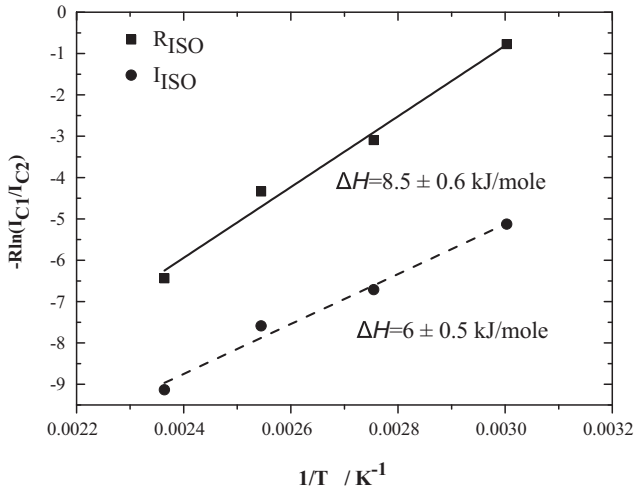

Fig. 7. Arrhenius type plots of the temperature dependence I_{C_1}/I_{C_2} intensities ratios as they derived from the Isotropic (●) and Reduced Isotropic (■) spectra values for the protic HMImTFSI ionic liquid. Dashed and solid lines represent the best linear fits.

4. Conclusions

The structural changes of the protic ionic liquid HMImTFSI occurring upon melting and at temperatures up to 150 °C were studied using vibrational spectroscopy (FT-Raman/FTIR). In the solid phase $TFSI^-$ adopts mainly the trans conformation while upon melting both the cis and trans conformers coexist. Also the ΔH of the equilibrium between the $TFSI^-$ rotamers was calculated from the reduced isotropic Raman spectra and was found ~8.5 kJ/mol. Furthermore, ion pairs are probably formed in the liquid phase. In these pairs the ions are connected mainly with HB through the N—H of the imidazolium ring and the O of $TFSI^-$.

Acknowledgements

The authors would like to acknowledge Prof. G.N. Papatheodorou and Dr. S.N. Yannopoulos for fruitful discussions on the manuscript. The authors would, also, like to acknowledge financial support from the European Commission through the FP7 funded program ZEOCELL (Grant Agreement no: 209481) and Solvionic S.A. for providing HMImTFSI. We also like to thank A. Chrissanthopoulos for the artwork of figure 1.

Appendix A. Supplementary data

Supplementary data associated with this article can be found, in the online version, at http://dx.doi.org/10.1016/j.vibspec.2012.08.006.

References

[1] C.A. Angell, N. Byrne, J.-P. Belieres, Phys. Chem. Appl. Acc. Chem. Res. 40 (2007) 1228.
[2] J.P. Hallett, T. Welton, Chem. Rev. (Washington, DC, U.S.) 111 (2011) 3508.
[3] N.V. Plechkova, K.R. Seddon, Chem. Soc. Rev. 37 (2008) 123.
[4] T. Welton, Chem. Rev. (Washington, DC, U.S.) 99 (1999) 2071.
[5] D. Zhao, M. Wu, Y. Kou, E. Min, Catal. Today 74 (2002) 157.
[6] H. Olivier-Bourbigou, L. Magna, D. Morvan, Appl. Catal. A: Gen. 373 (2010) 1.
[7] V.I. Pârvulescu, C. Hardacre, Chem. Rev. (Washington, DC, U.S.) 107 (2007) 2615.
[8] T. Welton, Coord. Chem. Rev. 248 (2004) 2459.
[9] J. Dupont, R.F. de Souza, P.A.Z. Suarez, Chem. Rev. (Washington, DC, U.S.) 102 (2002) 3667.
[10] P. Wasserscheid, W. Keim, Angew. Chem. Int. Ed. 39 (2000) 3772.
[11] F. van Rantwijk, R.A. Sheldon, Chem. Rev. (Washington, DC, U.S.) 107 (2007) 2757.
[12] U. Kragl, M. Eckstein, N. Kaftzik, Curr. Opin. Biotechnol. 13 (2002) 565.
[13] M.C. Buzzeo, R.G. Evans, R.G. Compton, ChemPhysChem 5 (2004) 1106.
[14] M. Galiński, A. Lewandowski, I. Stępniak, Electrochim. Acta 51 (2006) 5567.
[15] D.R. MacFarlane, M. Forsyth, Adv. Mater. (Weinheim, Germany) 13 (2001) 957.
[16] T. Torimoto, T. Tsuda, K-i. Okazaki, S. Kuwabata, Adv. Mater. (Weinheim, Germany) 22 (2010) 1196.
[17] M. Antonietti, D. Kuang, B. Smarsly, Y. Zhou, Angew. Chem. Int. Ed. 43 (2004) 4988.
[18] S.A. Shamsi, N.D. Danielson, J. Sep. Sci. 30 (2007) 1729.
[19] D. Bankmann, R. Giernoth, Prog. Nucl. Magn. Reson. Spectrosc. 51 (2007) 63.
[20] P. Siddharth, Anal. Chim. Acta 556 (2006) 38.
[21] M. Koel, Crit. Rev. Anal. Chem. 35 (2005) 177.
[22] F.P. Colin, J. Chromatogr. A 1037 (2004) 1.
[23] D.J. Couling, R.J. Bernot, K.M. Docherty, J.K. Dixon, E.J. Marginn, Green Chem. 8 (2006) 82.
[24] D. Coleman, N. Gathergood, Chem. Soc. Rev. 39 (2010) 600.
[25] R.P. Swatloski, J.D. Holbrey, R.D. Rogers, Green Chem. 5 (2003) 361.
[26] M. Deetlefs, K.R. Seddon, Green Chem. 12 (2010) 17.
[27] P.T. Anastas, J.C. Warner, Green Chemistry: Theory and Practice, Oxford University Press, Oxford, 1998.
[28] D. Kralisch, D. Reinhardt, G. Kreisel, Green Chem. 9 (2007) 1308.
[29] S.M. Urahata, M.C.C. Ribeiro, J. Chem. Phys. 120 (2004) 4.
[30] Y. Wang, G.A. Voth, J. Am. Chem. Soc. 127 (2005) 12192.
[31] Y. Wang, G.A. Voth, J. Phys. Chem. B 110 (2006) 18601.
[32] J.N.A. Canongia Lopes, A.A.H. Pádua, J. Phys. Chem. B 110 (2006) 3330.
[33] W. Jiang, Y. Wang, G.A. Voth, J. Phys. Chem. B 111 (2007) 4812.
[34] Y. Wang, W. Jiang, T. Yan, G.A. Voth, Acc. Chem. Res. 40 (2007) 1193.
[35] S. Shigeto, H-o. Hamaguchi, Chem. Phys. Lett. 427 (2006) 329.
[36] K. Iwata, H. Okajima, S. Saha, H.O. Hamaguchi, Acc. Chem. Res. 40 (2007) 1174.
[37] D. Xiao, J.R. Rajian, S. Li, R.A. Bartsch, E.L. Quitevis, J. Phys. Chem. B 110 (2006) 16174.
[38] D. Xiao, J.R. Rajian, A. Cady, S. Li, R.A. Bartsch, E.L. Quitevis, J. Phys. Chem. B 111 (2007) 4669.

[39] D. Xiao, J.R. Rajian, L.G. Hines, S. Li, R.A. Bartsch, E.L. Quitevis, J. Phys. Chem. B 112 (2008) 13316.
[40] A. Triolo, O. Russina, B. Fazio, G.B. Appetecchi, M. Carewska, S. Passerini, J. Chem. Phys. 130 (2009) 164521.
[41] L. Gontrani, O. Russina, F.L. Celso, R. Caminiti, G. Annat, A. Triolo, J. Phys. Chem. B 113 (2009) 9235.
[42] H. Ohno, M. Yoshizawa, Solid State Ionics 303 (2002) 154–155.
[43] T. Köddermann, C. Wertz, A. Heintz, R. Ludwig, ChemPhysChem 7 (2006) 1944.
[44] V. Kempter, B. Kirchner, J. Mol. Struct. 972 (2010) 22, and references therein.
[45] H. Nakamoto, A. Noda, K. Hayamizu, S. Hayashi, H-o. Hamaguchi, M. Watanabe, J. Phys. Chem. C 111 (2007) 1541.
[46] P.A. Hunt, J. Phys. Chem. B 111 (2007) 4844, and references therein.
[47] K. Fumino, A. Wulf, R. Ludwig, Angew. Chem. Int. Ed. 47 (2008) 8731.
[48] K. Noack, P.S. Schulz, N. Paape, J. Kiefer, P. Wasserscheid, A. Leipertz, Phys. Chem. Chem. Phys. 12 (2010) 14153.
[49] T.L. Greaves, C.J. Drummond, Chem. Rev. (Washington, DC, U.S.) 108 (2007) 206.
[50] V.N. Emel'yanenko, S.P. Verevkin, A. Heintz, K. Voss, A. Schulz, J. Phys. Chem. B 113 (2009) 9871.
[51] M. Yoshizawa, W. Xu, A. Angell, J. Am. Chem. Soc. 125 (2003) 15411.
[52] G.A. Luduena, T.D. Kuhne, D. Sebastiani, Chem. Mater. 23 (2011) 1424, and references therein.
[53] H. Tokuda, K. Hayamizu, K. Ishii, M.A.B.H. Susan, M. Watanabe, J. Phys. Chem. B 109 (2005) 6103.
[54] K. Fumino, A. Wulf, R. Ludwig, Phys. Chem. Chem. Phys. 11 (2009) 8790.
[55] S. Zahn, J. Thar, B. Kirchner, Chem. Phys. 132 (2010) 124506–124511.
[56] A. Martinelli, A. Matic, P. Johansson, P. Jacobsson, L. Börjesson, A. Fernicola, S. Panero, B. Scrosati, H. Ohno, J. Raman Spectrosc. 42 (2011) 522.
[57] O. Russina, A. Triolo, D. Xiao, L.G. Hines Jr., E.L. Quitevis, L. Gontrani, R. Caminiti, N.V. Plechkova, K.R. Seddon, J. Phys.: Condens. Matter 21 (2009) 424121.
[58] A. Triolo, O. Russina, H.-J. Bleif, E. Di Cola, J. Phys. Chem. B 111 (2007) 4641.
[59] A. Triolo, O. Russina, B. Fazio, R. Triolo, E. Di Cola, Chem. Phys. Lett. 457 (2008) 362.
[60] A. Triolo, O. Russina, B. Fazio, G.A. Appetecchi, M. Carewska, S. Passerini, J. Chem. Phys. 130 (16452) (2009).
[61] T. Peppel, C. Roth, K. Fumino, D. Paschek, M. Köckerling, R. Ludwig, Angew. Chem. Int. Ed. 50 (2011) 6661.
[62] M. Herstedt, M. Smirnov, P. Johansson, M. Chami, J. Grondin, L. Servant, J.C. Lassègues, J. Raman Spectrosc. 36 (2005) 762.
[63] K. Fujii, T. Fujimori, T. Takamuku, R. Kanzaki, Y. Umebayashi, S-i. Ishiguro, J. Phys. Chem. B 110 (2006) 8179.
[64] J.C. Lassègues, J. Grondin, R. Holomb, P. Johansson, J. Raman Spectrosc. 38 (2007) 551.
[65] M. Castriota, T. Caruso, R.G. Agostino, E. Cazzanelli, W.A. Henderson, S. Passerin, J. Phys. Chem. A 109 (2005) 13177.
[66] I. Rey, P. Johansson, J. Lindgren, J.C. Lassègues, J. Grondin, L. Servant, J. Phys. Chem. A 102 (1998) 3249.
[67] J. Kiefer, J. Fries, A. Leipertz, Appl. Spectrosc. 61 (2007) 1306.
[68] J. Grondin, J.C. Lassègues, D. Cavagnat, T. Buffeteau, P. Johansson, R. Holomb, J. Raman Spectrosc. 42 (2011) 733.
[69] D.A. Carter, J.E. Pemberton, J. Raman Spectrosc. 28 (1997) 939, and references therein.
[70] J. Foropoulos, D.D. DesMarteau, Inorg. Chem. 23 (1984) 3720.
[71] V. Deimede, G.A. Voyiatzis, J.K. Kallitsis, L. Qingfeng, N.J. Bjerrum, Macromolecules 33 (2000) 7609.
[72] D.J. Skrovanek, S.E. Howe, P.C. Painter, M.M. Coleman, Macromolecules 18 (1985) 1676.
[73] D.J. Skrovanek, P.C. Painter, M.M. Coleman, Macromolecules 19 (1986) 699.
[74] A. Martinelli, A. Matic, P. Jacobsson, L. Börjesson, A. Fernicola, S. Panero, B. Scrosati, H. Ohno, J. Phys. Chem. B 111 (2007) 12462.
[75] P. Musto, F.E. Karasz, W.J. MacKnight, Macromolecules 24 (1991) 4762.
[76] M. Xie, Y. Qi, Y. Hu, J. Phys. Chem. A 115 (2011) 3060.
[77] N.N. Chipanina, I.V. Sterkhova, T.N. Aksamentova, L.V. Sherstyannikova, V.A. Kukhareva, B.A. Shainyan, Rus. J. Gen. Chem. 78 (2008) 12.
[78] R.W. Berg, M. Deetlefs, K.R. Seddon, I. Shim, J.M. Thompson, J. Phys. Chem. B 109 (2005) 19018.
[79] G.N. Papatheodorou, S.N. Yannopoulos, in: M. Gaune-Escard (Ed.), Molten Salts: From Fundamentals to Applications, Kluwer Academic Publishers, 2002, 47 pp.
[80] J.C. Lassègues, J. Grondin, C. Aupetit, P. Johansson, J. Phys. Chem. A 113 (2009) 305.
[81] J.C. Lassègues, J. Grondin, D. Cavagnat, P. Johansson, J. Phys. Chem. A 113 (2009) 6419.
[82] C. Rerchard, A. Novak, Spectrochim. Acta 23A (1953) (1967).
[83] N. Heimer, R.E. Del Sesto, Z. Meng, John.S. Wilkes, W.R. Carper, J. Mol. Liq. 124 (2006) 84.
[84] D. Brouillette, D.E. Irish, N.J. Taylor, G. Perron, M. Odziemkowski, J.E. Desnoyers, Phys. Chem. Chem. Phys. 4 (2002) 6063.